Genomic signatures of evolutionary rescue in bats surviving white-nose syndrome

Sarah A. Gignoux-Wolfsohn [1*], Malin L. Pinsky [1], Kathleen Kerwin[1], Carl Herzog[2], MacKenzie Hall[3], Alyssa B. Bennett[4], Nina H. Fefferman[5,6], Brooke Maslo[1]

1 Department of Ecology, Evolution, and Natural Resources, Rutgers, The State University of New Jersey, New Brunswick, NJ USA
2 New York State Department of Environmental Conservation, Albany, NY USA
3 Endangered and Nongame Species Program, New Jersey Department of Environmental Protection, Trenton, NJ USA
4 Vermont Fish and Wildlife Department, Rutland, VT USA
5 Ecology and Evolutionary Biology, University of Tennessee, Knoxville, TN USA
6 National Institute for Mathematical and Biological Synthesis, University of Tennessee, TN USA

*corresponding author current address: Smithsonian Environmental Research Center, Edgewater, MD USA. Email: gw.sarah@gmail.com

Evolutionary rescue can in theory help populations avoid extinction after abrupt environmental change through the rapid evolution of advantageous traits that promote population growth [1,2]. However, evolutionary rescue is thought to be rare in taxa with long generation times because demographic declines towards extirpation are likely to outpace the acquisition of adaptive *de novo* mutations [3]. Adaptive alleles must therefore be selected from standing genetic variation, a process that leaves few detectable genomic signatures [4]. Here, we provide the first genetic evidence for evolutionary rescue in bat populations affected by white nose syndrome (WNS). By comparing genetic samples from before and after little brown bat populations were decimated by WNS, we identified signatures of soft selection on standing genetic variation. This selection occurred at multiple loci in genes linked to hibernation behavior, suggesting that changes in hibernation have allowed these bats to survive infection with WNS. Through these findings, we show that evolutionary rescue can be a conservation-relevant process even in slowly-reproducing taxa facing extinction.

Many North American bat species are currently facing extinction due to white-nose syndrome (WNS), an infectious disease caused by the introduced fungal pathogen, *Pseudogymnoascus destructans* [5-7]. *P. destructans* infects bats during hibernation; it creates

lesions in wing membranes, disrupts homeostasis, and depletes energy stores by increasing the frequency of arousal from torpor [5,8]. In spite of the risk of extinction, some remnant populations of one species, the little brown bat (*Myotis lucifugus*), have returned to positive growth in recent years after abundance declines of up to 98% [7,9], with some populations beginning to display the classic, U-shaped trajectory symbolic of evolutionary rescue [2]. Recent analyses of population declines and infection rates suggest that host resistance is the driving mechanism behind these population trajectories, rather than alternative mechanisms such as host tolerance, demographic compensation, or reduced pathogen virulence[10]. What remains unclear is whether this resistance results from adaptive immunity or from selection of genetically resistant individuals[11]. Only the latter mechanism is consistent with evolutionary rescue.

We performed low-coverage whole genome sequencing on 132 individuals from four hibernacula within the epicenter of WNS emergence (Northeastern US, Fig. 1a): two hibernacula, Hibernia Mine (*hereafter,* Hibernia) and Walter Williams Preserve (*hereafter,* Williams), were sampled both before infection by WNS (2008 and 2009, respectively) and after infection by WNS (2016); one hibernaculum, Greeley Mine (*hereafter* Greeley), was sampled pre-WNS (2008); and another, Aeolus Cave (*hereafter* Aeolus), was sampled post-WNS (Figure 1). We achieved an average depth of coverage of 2.42 +/- 1.24 (Supplementary Data Table 1) and used probabilistic methods to identify a total of 44,829,667 SNPs (Single Nucleotide Polymorphisms) and to calculate allele frequencies across the genome (see Methods).

We found little geographic structure at a genome-wide level, including low pairwise F_{ST} values (pre-WNS samples 0.0176 +/- 0.33×10^{-4}, post-WNS samples 0.0143 +/- 3.33×10^{-4}) and weak population structure that did not correspond to geographic populations (Fig. 2a, b). A lack of population structure is consistent with previous studies demonstrating near panmixia over evolutionary time in bat populations east of the Rocky Mountains [12,13] likely because relatively few bats moving between hibernacula are able to reduce population structure on an evolutionary timescale. In contrast, most bats have high fidelity to mating sites and hibernacula within a given generation[14]. Mark-recapture data collected at Hibernia over the last seven years reveals that 95% of bats banded there returned to this hibernaculum, with banded bats repeatedly recaptured from year to year. This ecological site fidelity indicated that allele dynamics were largely independent among the hibernacula over the one to two generations that have elapsed since WNS infection (Supplementary Data Tables 2 and 3). We found that our little brown bats may have

originated from two populations, with the vast majority of ancestry in nearly all bats coming from one evolutionary population. Two bats sampled at pre-WNS Williams may have originated from a second population. We removed these two bats from calculations of allele frequency change in Williams and Hibernia for the results we present in the main text (Figure 2b), but see Supplementary Data Figure 3 for sensitivity analyses with them included. We further found little temporal structure as a result of WNS (F_{ST} comparing pre-WNS population to post-WNS population, Hibernia: 0.016, Williams: 0.017), indicating that WNS did not affect population structure and that pre-WNS populations were not replaced by individuals from other populations (Fig. 2).

Demographic declines were dramatic at Hibernia (98% decline from 2009-2015 followed by a return to pre-WNS survival rates and a slow but positive population growth rate; Fig. 1b, Supplementary Information), while more moderate declines followed by recovery were observed at Williams (80% from 2008-2010 followed by recovery, see Fig. 1b). The rate of recovery may be tied to different initial population sizes, with the smaller Hibernia (26,438 individuals in 2009) recovering more slowly than Williams (87,401 individuals in 1999). Tajima's D is a genetic statistic that typically increases after a bottleneck as drift removes rare variants and then returns to its pre-bottleneck value as the population recovers [15]. Consistent with observed differences in population recovery, Tajima's D increased from pre- to post-WNS samples in the smaller and more heavily bottlenecked Hibernia population, but not in the relatively more abundant and rapidly recovering Williams population (Fig. 3).

If evolutionary rescue has occurred in little brown bat populations, we expect it would occur as a soft selective sweep from standing genetic variation because the short timescale of WNS infection, mortality, and recovery makes selection on novel mutations unlikely. Soft selection has only recently been acknowledged as a common and possibly dominant method of selection, though one that has been largely overlooked because of detection difficulty [16,17]. After comparing allele frequency changes in populations from Hibernia and Williams to a null model of genetic drift and sampling variance, we identified 85 SNPs at a false detection rate of 0.2 in both populations with significantly greater allele frequency changes than would be expected. These results were consistent with selection operating in parallel on SNPs in these two populations (Fig. 4a, b). The candidate SNPs were present at low to moderate frequencies in pre-WNS populations of both Hibernia and Williams and in low to intermediate frequencies at the

pre-WNS sample from Greeley mine (Fig. 4c). Post-WNS allele frequencies in Hibernia, Williams and Aeolus ranged from intermediate to high, suggesting incomplete selective sweeps at some loci and near-complete sweeps at others (Fig. 4d). However, pre-WNS frequencies at the candidate SNPs were highest in Williams and post-WNS frequencies were lowest at Aeolus, suggesting that while it is likely that there is concurrent selection occurring across multiple populations, selection is not acting to the same degree on the same loci at all populations affected by WNS. Such signatures are consistent with soft selection for traits controlled by many loci [17]. As further evidence against hard selection, genomic regions surrounding SNPs putatively under selection did not show classic signatures of hard selection (changes in π and Tajima's D, Supplementary Data Figs. 1 and 2).

We further tested whether parallel changes in allele frequencies across Hibernia and Williams could be explained by dispersal between populations. However, we found that migrating individuals would have to make up >52% of each population, while <0.02% of bats at Williams (out of 16,000) have been found migrating from Hibernia and no bats from Williams have been found at Hibernia (Supplementary Data Tables 2 and 4). This result suggests that selection acted *in situ* and independently in each population.

Twenty-one of the 85 candidate SNPs under selection were located in annotated regions (Supplementary Data Table 5). These SNPs were all located in presumed introns. Introns can play important regulatory roles, and mutations in introns have been associated with numerous diseases [18]. Introns have a higher mutation rate due to lower evolutionary constraint and may be good candidates for selection on standing genetic variation. Functional annotation strongly suggested that selection has acted on hibernation behavior, with most (15 of 21) annotated genes involved in regulating processes associated with hibernation. Two genes (ABAT and BMAL1) are depressed during torpor and overexpressed upon arousal from torpor in ground squirrels[19]. Another gene previously associated with ground squirrel hibernation (EXOC4) [20] had a SNP with temporal allele frequency changes greater than 0.45 in both Hibernia and Williams populations, low frequency in (pre-WNS) Greely and high frequency in (post-WNS) Aeolus. Other genes (MDAG2[21], SORCS3[22], PCDH17[23], MKL2[24], Kremen1[25]) were associated with neural regeneration and plasticity and likely regulate the neural changes involved in hibernating mammals: shrinking of neurons, inhibition of neurogenesis, and reduction of synapses, all of which are rapidly reversed upon arousal from hibernation [26]. Many of these genes have been

associated with human neurodegenerative diseases like Parkinson's, Alzheimer's, and neuratypical phenotypes (Supplementary Data Table 5). Hibernating mammals have also been proposed as a model system for both reversible neurodegenerative diseases [27] and neuroprotection [28].

In addition to neural changes, hibernating bats undergo significant changes in fat accumulation and metabolism leading up to and during torpor [29]. We identified several SNPs in genes associated with insulin regulation and fat accumulation (GNPDA1 [30], REPS2 [31], SOX5 [32], ADCY3 [33], CMIP[34]). These genes are likely involved in regulating changes in insulin levels throughout the hibernation cycle [35], which mimics the pathology of type 2 diabetes [36]. Contrary to other studies of disease-induced selection (e.g., [37]), we found only one SNP in a gene that is involved in immune system function (MASP1, part of the complement pathway). Further work will be needed to directly link these genetic changes to changes in gene expression and hibernation phenotypes.

When hibernating bats are infected with *P. destructans*, the frequency of torpor arousal increases, which prematurely depletes fat stores and leads to mortality [8,38]. Selection for hibernation-related genes in this host-pathogen system is therefore a logical but unintuitive consequence of WNS infection. Disease-induced arousal may be a failed attempt to fight off the pathogen by re-activating the immune system [39], but an increased immune response and production of anti-*P. destructans* antibodies is not correlated with survival and is therefore likely only reducing energy reserves [40]. Furthermore, European bats that harbor *P. destructans* but do not display signs of WNS frequently have lower levels of anti-*P. destructans* antibodies than uninfected bats [41]. Our results suggest that changes in hibernation behavior are the key to host survival, and that evolutionary rescue has altered hibernation behavior in little brown bats. Intriguingly, big brown bats (*Eptesicus fuscus*), which have suffered much smaller population declines, increase their torpor duration when exposed to *P. destructans* [42].

By accounting for changes in allele frequency due to drift, we have employed a statistically robust method to identify soft selective events when genetic data are available from multiple timepoints. We were therefore able to detect selection that would otherwise have been nearly invisible [4]. Characterizing the full suite of adaptive alleles present will require detecting SNPs likely under selection in other populations given that stochastic variability in pre-WNS genetic variation determines which alleles are available for selection.

Our findings that some WNS-affected little brown bat populations have returned to positive growth and that remnant populations have genetic differences associated with hibernation behavior suggest that evolved changes in hibernation behavior have allowed these remnant bats to survive exposure to *P. destructans*. These surviving individuals have the potential to rescue little brown bat populations and ultimately return them to stable population levels[11]. Unexpectedly, the genomic mechanisms of evolutionary rescue in bats appear relevant to efforts to understand and treat Parkinson's, Alzheimer's, and diabetes, suggesting that studies of WNS tolerant or resistant bats could offer new perspectives on these diseases. Management decisions (*e.g.,* whether to deploy treatments for *P. destructans* or protect populations from other detrimental forces) can be informed by knowing the frequency of resistant individuals in both uninfected and infected populations. The deployment of vaccines or treatments for *P. destructans* may be needed only in populations with low evolutionary potential[17]. Our finding that WNS likely induced evolutionary rescue in this species suggests that evolutionary rescue may be occurring in other instances of pathogen-induced selection (*e.g*., [43]).

Acknowledgements

The authors would like to thank Nina Therkildsen, Noah Rose, and Michelle Stuart for help with troubleshooting; Lisa Komoroske, Jennifer Hoey, Katrina Catalano, and Erik Holum for numerous discussions about data analyses. We thank Brian Schumm and multiple other field personnel for assistance in sampling bats. Funding for this project was provided through United States Fish and Wildlife Service Grant F15AP00949.

References

1 Gonzalez, A., Ronce, O., Ferriere, R. & Hochberg, M. E. Evolutionary rescue: an emerging focus at the intersection between ecology and evolution. *Philosophical transactions of the Royal Society of London. Series B, Biological sciences* **368**, 20120404, doi:10.1098/rstb.2012.0404 (2013).

2 Vander Wal, E., Garant, D., Festa-Bianchet, M. & Pelletier, F. Evolutionary rescue in vertebrates: evidence, applications and uncertainty. *Philosophical transactions of the Royal Society of London. Series B, Biological sciences* **368**, 20120090, doi:10.1098/rstb.2012.0090 (2013).

3 Carlson, S. M., Cunningham, C. J. & Westley, P. A. Evolutionary rescue in a changing world. *Trends Ecol Evol* **29**, 521-530, doi:10.1016/j.tree.2014.06.005 (2014).

4 Przeworski, M., Coop, G. & Wall, J. D. The Signature of Positive Selection on Standing Genetic Variation. *Evolution; international journal of organic evolution* **59**, 2312, doi:10.1554/05-273.1 (2005).

5 Gargas, A., Trest, M. T., Christensen, M., Volk, T. J. & Blehert, D. S. Geomyces destructans sp. nov. associated with bat white-nose syndrome. *Mycotaxon* **108**, 147-154 (2009).

6 Frick, W. F. *et al.* Disease alters macroecological patterns of North American bats. *Global Ecology and Biogeography* **24**, 741-749 (2015).

7 Frick, W. F. *et al.* An emerging disease causes regional population collapse of a common North American bat species. *Science* **329**, 679-682, doi:10.1126/science.1188594 (2010).

8 Reeder, D. M. *et al.* Frequent arousal from hibernation linked to severity of infection and mortality in bats with white-nose syndrome. *PLoS One* **7**, e38920, doi:10.1371/journal.pone.0038920 (2012).

9 Maslo, B., Valent, M., Gumbs, J. F. & Frick, W. Conservation implications of ameliorating survival of little brown bats with white-nose syndrome. *Ecological Applications* **25**, 1832-1840 (2015).

10 Langwig, K. E. *et al.* Resistance in persisting bat populations after white-nose syndrome invasion. *Philosophical transactions of the Royal Society of London. Series B, Biological sciences* **372**, doi:10.1098/rstb.2016.0044 (2017).

11 Maslo, B. & Fefferman, N. H. A case study of bats and white-nose syndrome demonstrating how to model population viability with evolutionary effects. *Conservation biology : the journal of the Society for Conservation Biology* **29**, 1176-1185, doi:10.1111/cobi.12485 (2015).

12 Wilder, A. P., Kunz, T. H. & Sorenson, M. D. Population genetic structure of a common host predicts the spread of white-nose syndrome, an emerging infectious disease in bats. *Molecular ecology* **24**, 5495-5506, doi:10.1111/mec.13396 (2015).

13 Vonhof, M. J., Amelon, S. K., Currie, R. R. & McCracken, G. F. Genetic structure of winter populations of the endangered Indiana bat (Myotis sodalis) prior to the white nose syndrome epidemic: implications for the risk of disease spread. *Conservation Genetics* **17**, 1025-1040, doi:10.1007/s10592-016-0841-6 (2016).

14 Norquay, K. J. O., Martinez-Nuñez, F., Dubois, J. E., Monson, K. M. & Willis, C. K. R. Long-distance movements of little brown bats (*Myotis lucifugus*). *Journal of Mammalogy* **94**, 506-515, doi:10.1644/12-mamm-a-065.1 (2013).

15 Tajima. The Effect of Change in Population Size on DNA Polymorphism. *Genetics* **123**, 597-601 (1989).

16 Schrider, D. R. & Kern, A. D. Soft Sweeps Are the Dominant Mode of Adaptation in the Human Genome. *Mol Biol Evol* **34**, 1863-1877, doi:10.1093/molbev/msx154 (2017).
17 Messer, P. W. & Petrov, D. A. Population genomics of rapid adaptation by soft selective sweeps. *Trends Ecol Evol* **28**, 659-669, doi:10.1016/j.tree.2013.08.003 (2013).
18 Ma, M. *et al.* Disease-associated variants in different categories of disease located in distinct regulatory elements. *BMC genomics* **16** (2015).
19 Yan, J., Barnes, B. M., Kohl, F. & Marr, T. G. Modulation of gene expression in hibernating arctic ground squirrels. *Physiological genomics* **32**, 170-181, doi:10.1152/physiolgenomics.00075.2007 (2008).
20 Grabek, K. R. *et al.* Genetic architecture drives seasonal onset of hibernation in the 13-lined ground squirrel. doi:10.1101/222307 (2017).
21 Joset, P. *et al.* Rostral growth of commissural axons requires the cell adhesion molecule MDGA2. *Neural Development* **6** (2011).
22 Christiansen, G. B. *et al.* The sorting receptor SorCS3 is a stronger regulator of glutamate receptor functions compared to GABAergic mechanisms in the hippocampus. *Hippocampus* **27**, 235-248, doi:10.1002/hipo.22689 (2017).
23 Hirano, S., Suzuki, S. & Redies, C. The Cadherin Superfamily in Neural Development: Diversity, Funciton and Interaction with Other Molecules. *Frontiers in Bioscience* **8**, 306-356 (2003).
24 Kaneda, M. *et al.* Synaptic localisation of SRF coactivators, MKL1 and MKL2, and their role in dendritic spine morphology. *Scientific reports* **8**, 727, doi:10.1038/s41598-017-18905-7 (2018).
25 Wu, D. & Murashov, A. K. MicroRNA-431 regulates axon regeneration in mature sensory neurons by targeting the Wnt antagonist Kremen1. *Front Mol Neurosci* **6**, 35, doi:10.3389/fnmol.2013.00035 (2013).
26 Leon-Espinosa, G. *et al.* Decreased adult neurogenesis in hibernating Syrian hamster. *Neuroscience* **333**, 181-192, doi:10.1016/j.neuroscience.2016.07.016 (2016).
27 Braidy, N. *et al.* Recent rodent models for Alzheimer's disease: clinical implications and basic research. *J Neural Transm (Vienna)* **119**, 173-195, doi:10.1007/s00702-011-0731-5 (2012).
28 Zhou, F. *et al.* Hibernation, a Model of Neuroprotection. *American Journal of Pathology* **158** (2001).
29 Carey, H. V., Andrews, M. T. & Martin, S. L. Mammalian Hibernation: Cellular and molecular Responses to Depressed Metabolism and Low Temperature. *Physiol Rev* **83**, 1153-1181 (2003).
30 Kotnik, P. *et al.* Identification of novel alleles associated with insulin resistance in childhood obesity using pooled-DNA genome-wide association study approach. *International Journal of Obesity* **42**, 686-695, doi:10.1038/ijo.2017.293 (2018).
31 Badway, J. A. & Baleja, J. D. Reps2: A cellular signaling and molecular trafficking nexus. *The International Journal of Biochemistry & Cell Biology* **43**, 1660-1663, doi:10.1016/j.biocel.2011.08.014 (2011).
32 Axelsson, A. S. *et al.* Sox5 regulates beta-cell phenotype and is reduced in type 2 diabetes. *Nature communications* **8**, 15652, doi:10.1038/ncomms15652 (2017).
33 Grarup, N. *et al.* Loss-of-function variants in ADCY3 increase risk of obesity and type 2 diabetes. *Nature genetics* **50**, 172-174, doi:10.1038/s41588-017-0022-7 (2018).

34 Keaton, J. M. *et al.* Genome-wide interaction with the insulin secretion locus MTNR1B reveals CMIP as a novel type 2 diabetes susceptibility gene in African Americans. *Genet Epidemiol* **42**, 559-570, doi:10.1002/gepi.22126 (2018).

35 Bauman, W. A. Seasonal Changes in Pancreatic Insulin and Glucagon in the Little Brown Bat *Pancreas* **5**, 342-346 (1990).

36 Wu, C. W., Biggar, K. K. & Storey, K. B. Biochemical adaptations of mammalian hibernation: exploring squirrels as a perspective model for naturally induced reversible insulin resistance. *Brazilian Journal of Medical and Biological Research* **46**, 1-13, doi:10.1590/1414-431x20122388 (2013).

37 Epstein, B. *et al.* Rapid evolutionary response to a transmissible cancer in Tasmanian devils. *Nature communications* **7**, 12684, doi:10.1038/ncomms12684 (2016).

38 Verant, M. L. *et al.* White-nose syndrome initiates a cascade of physiological disturbances in the hibernating bat host. *BMC Physiology* **14** (2014).

39 Storey, K. B. & Storey, J. M. in *Functional Metabolism: Regulation and Adaptation* (ed K. B. Storey) (John Wiley & Sons, 2004).

40 Lilley, T. M. *et al.* Immune responses in hibernating little brown myotis (Myotis lucifugus) with white-nose syndrome. *Proceedings of the Royal Society B: Biological Sciences* **284**, 20162232, doi:10.1098/rspb.2016.2232 (2017).

41 Johnson, J. S. *et al.* Antibodies toPseudogymnoascus destructansare not sufficient for protection against white-nose syndrome. *Ecology and evolution* **5**, 2203-2214, doi:10.1002/ece3.1502 (2015).

42 Moore, M. S. *et al.* Energy Conserving Thermoregulatory Patterns and Lower Disease Severity in a Bat Resistant to the Impacts of White-Nose Syndrome. *J Comp Physiol B* **188**, 163-176, doi:10.1007/s00360-017-1109-2) (2018).

43 Schiebelhut, L. M., Puritz, J. B. & Dawson, M. N. Decimation by sea star wasting disease and rapid genetic change in a keystone species,Pisaster ochraceus. *Proceedings of the National Academy of Sciences*, 201800285, doi:10.1073/pnas.1800285115 (2018).

Figure Legends

Figure 1. **Four hibernacula were sampled across time and are experiencing different rates of population recovery.** a) Location of hibernacula sampled in Northeast United States. b) population trajectories for Williams and Hibernia hibernacula, color coded according to 1a. Vertical lines represent the time of initial population decline due to WNS for each hibernaculum (color coded by hibernaculum). The dotted line represents missing data (population estimates for Williams were not taken between 1999 and 2010, 1999 is the presumed pre-WNS baseline). Triangles indicate sampling points for each hibernaculum, color coded.

Figure 2. **Population structure of little brown bats in the northeastern United States does not correspond to geography or time.** a) PCA plot shows a lack of population structure in the majority of individuals, with four potential outlier bats. B) Admixture plot showing k=2, the most likely k value. Colors denote different inferred ancestral origin populations. The four outliers from the PCA are marked at the top of the Admixture plots.

Figure 3. Change in Tajima's D reflects differences in population declines in Hibernia and Williams. Density plots of Tajima's D calculated in sliding windows across the genome in a) Hibernia mine and b) Williams mine from samples pre (solid line) and post (dotted line) infection with WNS. Mean Tajima's D across the entire genome is noted for each hibernaculum.

Figure 4. SNPs with signals of soft selection were located throughout the genome, were present at low to intermediate frequencies prior to WNS infection, and swept to incomplete or nearly complete fixation after WNS. a) Average change in allele frequency between pre and post-WNS samples from Hibernia and Williams. Scaffolds are closest approximations of chromosomes in MyoLuc 2.0 assembly. Significant SNPs (FDR=0.2) are highlighted in red. b) –log10 P values for SNPs with a positive change in allele frequency greater than 0.5 in both Hibernia and Williams and c) with a negative change in allele frequency greater than 0.5. Significant SNPS are highlighted in red. d) Density plots of allele frequencies for significant candidate SNPs (solid lines) and random SNPs (dotted lines) at each site pre-WNS and e) post-WNS.

Methods

Sample collection

We collected samples at two timepoints, before (pre-WNS) and after (post-WNS) disease-induced population declines. We collected pre-WNS samples from frozen specimens collected in the first year of disease emergence at Walter Williams Preserve, Ulster County, New York (2008); Hibernia Mine (HM), Morris County, New Jersey (2009); and Greeley Mine, Windsor County, Vermont (2009). We collected post-WNS samples from live individuals within the remnant populations at Hibernia Mine and Walter Williams Preserve, and from Aeolus Cave (Bennington County, Vermont) in 2016. At the time of post-WNS sampling, Greeley Mine was inaccessible. Sample collection followed [1]: briefly, a 2-mm wing tissue biopsy was taken (Miltex) and placed in RNALater (Ambion). Samples were collected under IACUC Protocol#: 15-068 and appropriate state permits.

Library preparation and sequencing

DNA was extracted using the QIAGEN Blood and Tissue kit, with the addition of RNase A to remove RNA contamination and following recommendations to increase the concentration of DNA (10 min elution step, smaller volume of elution buffer). Fragmented DNA was identified using 1.5% gel electrophoresis and when fragments <1 kbp were present, a cleanup step was performed with AMPure XP beads (Agencourt). DNA concentration was measured using a Qubit HS DNA Assay (Invitrogen).

Library prep was performed using the Illumina Nextera kit following the protocol developed by [2], modified from [3]. Briefly, samples were fragmented and adapters were added using tagmentase in a 2.5 µl volume. Because the ideal concentration of DNA given the size of the *M. lucifugus* genome was determined to be 10 ng/µl, which was below the concentration for many of our samples, we added an additional step to dilute the tagmentase for low concentration samples using 10xTB.

A two-step PCR procedure was then conducted using the KAPA Library Amplification kit and the Nextera index kit (primers N517—N504 and N701-N706) with a total of 12 cycles (8+4) to add a unique combination of barcodes to each sample and amplify the resulting libraries. We then purified and size selected these products with AMPure XP beads, quantified the

concentration of each library using the Qubit and examined the fragment size using an Agilent BioAnalyzer chip. Finally, we pooled the resulting libraries together in equal concentrations by mass. These pools were sequenced in 7 rapid runs (each of 2 lanes/run) on the Illumina HiSeq 2500 at the Princeton University Lewis-Siegler Institute.

Bioinformatics

All scripts and notebooks can be found at https://github.com/sagw/WNS_WGS/

To remove exact duplicate sequences (likely optical duplicates), we ran FastUniq in paired-end mode. We then used Trimmomatic v0.36 in paired-end mode to remove Illumina adapters, throw out reads with an average phred score below 33, trim any reads where a 4 basepair sliding window phred score fell below 15, and discard trimmed reads shorter than 30 basepairs.

We filtered contaminant sequences using fastqscreen v0.95 (https://www.bioinformatics.babraham.ac.uk/projects/fastq_screen/) with Bowtie2. Reads were screened against the human genome (ch38), all bacterial genomes, all fungal genomes including *P. destructans*, and all viral genomes available from NCBI (ftp://ftp.ncbi.nlm.nih.gov/genomes/genbank/). All reads were tagged for contaminants using fastqscreen. Less than 10% of reads were removed from unpaired reads using fastqscreen in filter mode and from paired reads using a custom script (/Scripts/pfilter.py).

We mapped resulting paired and unpaired reads to the *Myotis lucifugus* 2.0 genome (ftp://ftp.ensembl.org/pub/release-87/fasta/myotis_lucifugus/dna/) using Bowtie2 in very sensitive local mode [4].We then sorted sam files, converted to bam, and removed duplicate sequences using Picard (https://broadinstitute.github.io/picard/) (MarkDuplicates). We used Bedtools [5] to calculate percent coverage and discarded samples with reads that covered <20% of the genome. These filters resulted in 132 samples with an average coverage of 0.5x. Finally, we used GEM [6] to determine mappability of the reference genome. Only regions with a mappability score of 1 were used (1.7 out of 2.2 gigabases).

SNP calling and summary statistics

We called SNPs over all samples using ANGSD (v0.92) with the following parameters: the samtools model was used to estimate genotype likelihoods from the mapped reads (-GL 1), major and minor alleles and frequency were estimated from genotype likelihoods (-doMaf 1 -

doMajorMinor 1). We used the following quality filters (requires -doCounts 1): a minimum quality score of 20, minimum mapping score of 30, minimum number of individuals with data of 68 and max depth over all individuals of 1320. We used a cut-off p value of 10^{-6} (Likelihood Ratio Test). See /Notebooks/Angsd_all_SNPs for details.

We calculated genotype likelihoods for called SNPs with ANGSD in beagle format (-doGlf 2). These likelihoods were used to create a PCA, perform admixture analysis, and determine the most likely k value with PCAngsd[7], both visualized using R (see /Notebooks/Angsd_all_PCA_graphs).

In order to calculate FST between subpopulations, we first calculated unfolded sample allele frequencies with ANGSD using the reference genome to polarize the alleles for each subpopulation (-doSaf 1). We then created the following joint site frequency spectra with the angsd program realSFS: Hibernia pre-post, Williams pre-post, Hibernia-Williams-Greeley pre, Hibernia-Williams-Aeolus post. An average FST was calculated across the entire genome and in a sliding window across the genome. See /Notebooks/Angsd_all_FST.

We used the per-population sample allele frequencies to create unfolded site frequency spectra for each population. The sample allele frequencies and site frequency spectra were then used to calculate θ (population mutation rate) across the genome (-doThetas 1), and then calculate θ_w, π, and Tajima's D both across the genome and in a sliding window with the ANGSD program thetaStat (do_stat -win 1000 -step 1 -type 1). See /Notebooks/Angsd_all_thetas.

We estimated minor allele frequencies for each called SNP in each subpopulation using the previously inferred major and minor alleles (-doMajorMinor 3). Allele frequency was summed over 3 possible minor alleles weighted by probabilities (-doMaf 2). Maximum depth was set at 270. See /Notebooks/Angsd_all_SNPs.

Identifying SNPs putatively under selection

For the Hibernia and Williams colonies (excluding outlier bats, see Figure 1), change in minor allele frequency was calculated from mafs (method 2) as maf_{post}-maf_{pre}. We considered SNPs with a high change in allele frequency as those with changes greater than 0.5 or less than -0.5 in both Hibernia and Williams (in the same direction). To separate SNPs with high allele frequency changes due to sampling error or genetic drift from those under selection, we

developed locus-specific null models for allele frequency change. We first accounted for sampling error by using ANGSD to calculate minor allele frequencies from 100 bootstrapped file lists for Hibernia pre-WNS and post-WNS and Williams pre-WNS and post-WNS. Wright-Fisher simulations (1000 for each value) were then performed to estimate genetic drift [8,9]. We assumed 2 generations and effective population sizes of 424 and 296 (calculated using Hibernia census data, the smaller population size was used to be conservative). P-values were calculated for each SNP as p=r+1/n+1, where r was the number of times the simulated allele frequencies were greater than sampled bootstrapped allele frequencies, and n was the total number of simulations [68].

Because there is no evidence of significant bat migration between colonies in the time frame of this study (even if populations were panmictic in evolutionary time), the NJ and NY populations were considered independent and combined p values were calculated using the sum log method in the R package metap. The immigration required to achieve the observed allele frequency changes was calculated as % immigrants = 100*((Fpost1- Fpre1)/(Fpost2- Fpre1)), where Fpre1 was allele frequency in population 1 post-WNS, Fpre1 was allele frequency in population 1 pre-WNS, Fpost2 was allele frequency in population 2 post-WNS,. To account for multiple hypothesis testing, significance was then determined using the Benjamini-Hochberg method. Values were ranked from smallest to largest and the largest p value with the p <(i/m)Q was used as the significance cut off, where i was rank, m was the number of SNPs in both NJ and NY, and Q was the false discovery rate of 0.15.

The NCBI *Myotis Lucifugus* Annotation Release 102 was used to identify putative genes that contained the candidate SNPs and the Ensembl Variant Effect predictor was used to identify the location of SNPs within genes.

Methods References

1 Simmons, N. B. J. S. A. BIOLOGY-Taking Wing-Fossil and genetic findings elucidate the evolution of bats--And settle a long-standing debate over the origins of flight and echolocation. 96 (2008).

2 Therkildsen, N. O. & Palumbi, S. R. Practical low-coverage genomewide sequencing of hundreds of individually barcoded samples for population and evolutionary genomics in nonmodel species. *Mol Ecol Resour*, doi:10.1111/1755-0998.12593 (2016).

3 Baym, M. *et al.* Inexpensive multiplexed library preparation for megabase-sized genomes. *PLoS One* **10**, e0128036, doi:10.1371/journal.pone.0128036 (2015).

4 Langmead, B. & Salzberg, S. L. Fast gapped-read alignment with Bowtie 2. *Nature methods* **9**, 357-359, doi:10.1038/nmeth.1923 (2012).

5 Quinlan, A. R. & Hall, I. M. BEDTools: a flexible suite of utilities for comparing genomic features. *Bioinformatics* **26**, 841-842, doi:10.1093/bioinformatics/btq033 (2010).

6 Derrien, T. *et al.* Fast computation and applications of genome mappability. *PLoS One* **7**, e30377, doi:10.1371/journal.pone.0030377 (2012).

7 Meisner, J. & Albrechtsen, A., doi:10.1101/302463 (2018).

8 Fisher, R. A. On the Dominance Ratio. *Proceedings of the Royal Society Edinburgh* **42**, 321-431 (1922).

9 Wright, S. Evolution in Mendelian Populatins. *Genetics* **2**, 97-159 (1930).

10 Welinder, K. G. *et al.* Biochemical Foundations of Health and Energy Conservation in Hibernating Free-ranging Subadult Brown Bear Ursus arctos. *J Biol Chem* **291**, 22509-22523, doi:10.1074/jbc.M116.742916 (2016).

11 Joset, P. *et al.* Rostral growth of commissural axons requires the cell adhesion molecule MDGA2. *Neural Development* **6** (2011).

12 Connor, S. A. *et al.* Altered Cortical Dynamics and Cognitive Function upon Haploinsufficiency of the Autism-Linked Excitatory Synaptic Suppressor MDGA2. *Neuron* **91**, 1052-1068, doi:10.1016/j.neuron.2016.08.016 (2016).

13 Pettem, K. L., Yokomaku, D., Takahashi, H., Ge, Y. & Craig, A. M. Interaction between autism-linked MDGAs and neuroligins suppresses inhibitory synapse development. *J Cell Biol* **200**, 321-336, doi:10.1083/jcb.201206028 (2013).

14 Kotnik, P. *et al.* Identification of novel alleles associated with insulin resistance in childhood obesity using pooled-DNA genome-wide association study approach. *International Journal of Obesity* **42**, 686-695, doi:10.1038/ijo.2017.293 (2018).

15 Badway, J. A. & Baleja, J. D. Reps2: A cellular signaling and molecular trafficking nexus. *The International Journal of Biochemistry & Cell Biology* **43**, 1660-1663, doi:10.1016/j.biocel.2011.08.014 (2011).

16 Hoshina, N. *et al.* Protocadherin 17 Regulates Presynaptic Assembly in Topographic Corticobasal Ganglia Circuits. *Neuron* **78**, 839-854, doi:10.1016/j.neuron.2013.03.031 (2013).

17 Hirano, S., Suzuki, S. & Redies, C. The Cadherin Superfamily in Neural Development: Diversity, Funciton and Interaction with Other Molecules. *Frontiers in Bioscience* **8**, 306-356 (2003).

18 Chang, H. *et al.* The protocadherin 17 gene affects cognition, personality, amygdala structure and function, synapse development and risk of major mood disorders. *Mol Psychiatry* **23**, 400-412, doi:10.1038/mp.2016.231 (2018).

19 Axelsson, A. S. *et al.* Sox5 regulates beta-cell phenotype and is reduced in type 2 diabetes. *Nature communications* **8**, 15652, doi:10.1038/ncomms15652 (2017).

20 Kruer, M. C. *et al.* Defective FA2H leads to a novel form of neurodegeneration with brain iron accumulation (NBIA). *Annals of Neurology* **68**, 611-618, doi:10.1002/ana.22122 (2010).

21 Schneider, S. A. & Bhatia, K. P. Three faces of the same gene: FA2H links neurodegeneration with brain iron accumulation, leukodystrophies, and hereditary spastic paraplegias. *Annals of Neurology* **68** (2010).

22 Stergiakouli, E. *et al.* Genome-wide association study of height-adjusted BMI in childhood identifies functional variant in ADCY3. *Obesity (Silver Spring)* **22**, 2252-2259, doi:10.1002/oby.20840 (2014).

23 Saeed, S. *et al.* Loss-of-function mutations in ADCY3 cause monogenic severe obesity. *Nature genetics* **50**, 175-179, doi:10.1038/s41588-017-0023-6 (2018).

24 Grarup, N. *et al.* Loss-of-function variants in ADCY3 increase risk of obesity and type 2 diabetes. *Nature genetics* **50**, 172-174, doi:10.1038/s41588-017-0022-7 (2018).

25 Zhang, X., Zara, J., Siu, R. K., Ting, K. & Soo, C. The Role of NELL-1, a Growth Factor Associated with Craniosynostosis, in Promoting Bone Regeneration. *Journal of Dental Research* **89**, 865-878, doi:10.1177/0022034510376401 (2010).

26 Doty, S. B. & Nunez, E. A. Activation of Osteoclasts and the Repopulation of Bone Surfaces Following Hibernation in the Bat, Myotis lucifugus. *The Anatomical Record* **213**, 481-495 (1985).

27 Christiansen, G. B. *et al.* The sorting receptor SorCS3 is a stronger regulator of glutamate receptor functions compared to GABAergic mechanisms in the hippocampus. *Hippocampus* **27**, 235-248, doi:10.1002/hipo.22689 (2017).

28 Breiderhoff, T. *et al.* Sortilin-related receptor SORCS3 is a postsynaptic modulator of synaptic depression and fear extinction. *PLoS One* **8**, e75006, doi:10.1371/journal.pone.0075006 (2013).

29 Kaneda, M. *et al.* Synaptic localisation of SRF coactivators, MKL1 and MKL2, and their role in dendritic spine morphology. *Scientific reports* **8**, 727, doi:10.1038/s41598-017-18905-7 (2018).

30 Qu, L. *et al.* Association between polymorphisms in RAPGEF1, TP53, NRF1 and type 2 diabetes in Chinese Han population. *Diabetes Res Clin Pract* **91**, 171-176, doi:10.1016/j.diabres.2010.11.019 (2011).

31 Radha, V., Rajanna, A., Gupta, R. K., Dayma, K. & Raman, T. The guanine nucleotide exchange factor, C3G regulates differentiation and survival of human neuroblastoma cells. *Journal of Neurochemistry* **107**, 1424-1435, doi:10.1111/j.1471-4159.2008.05710.x (2008).

32 Keaton, J. M. *et al.* Genome-wide interaction with the insulin secretion locus MTNR1B reveals CMIP as a novel type 2 diabetes susceptibility gene in African Americans. *Genet Epidemiol* **42**, 559-570, doi:10.1002/gepi.22126 (2018).

33 Melvin, R. G. & Andrews, M. T. Torpor induction in mammals: recent discoveries fueling new ideas. *Trends in Endochrinology and Metabolism* **20**, doi:10.1016/j.tem.2009.09.005 (2009).

34 Yan, J., Barnes, B. M., Kohl, F. & Marr, T. G. Modulation of gene expression in hibernating arctic ground squirrels. *Physiological genomics* **32**, 170-181, doi:10.1152/physiolgenomics.00075.2007 (2008).

35 Wu, D. & Murashov, A. K. MicroRNA-431 regulates axon regeneration in mature sensory neurons by targeting the Wnt antagonist Kremen1. *Front Mol Neurosci* **6**, 35, doi:10.3389/fnmol.2013.00035 (2013).

36 Ross, S. P. *et al.* miRNA-431 Prevents Amyloid-beta-Induced Synapse Loss in Neuronal Cell Culture Model of Alzheimer's Disease by Silencing Kremen1. *Front Cell Neurosci* **12**, 87, doi:10.3389/fncel.2018.00087 (2018).

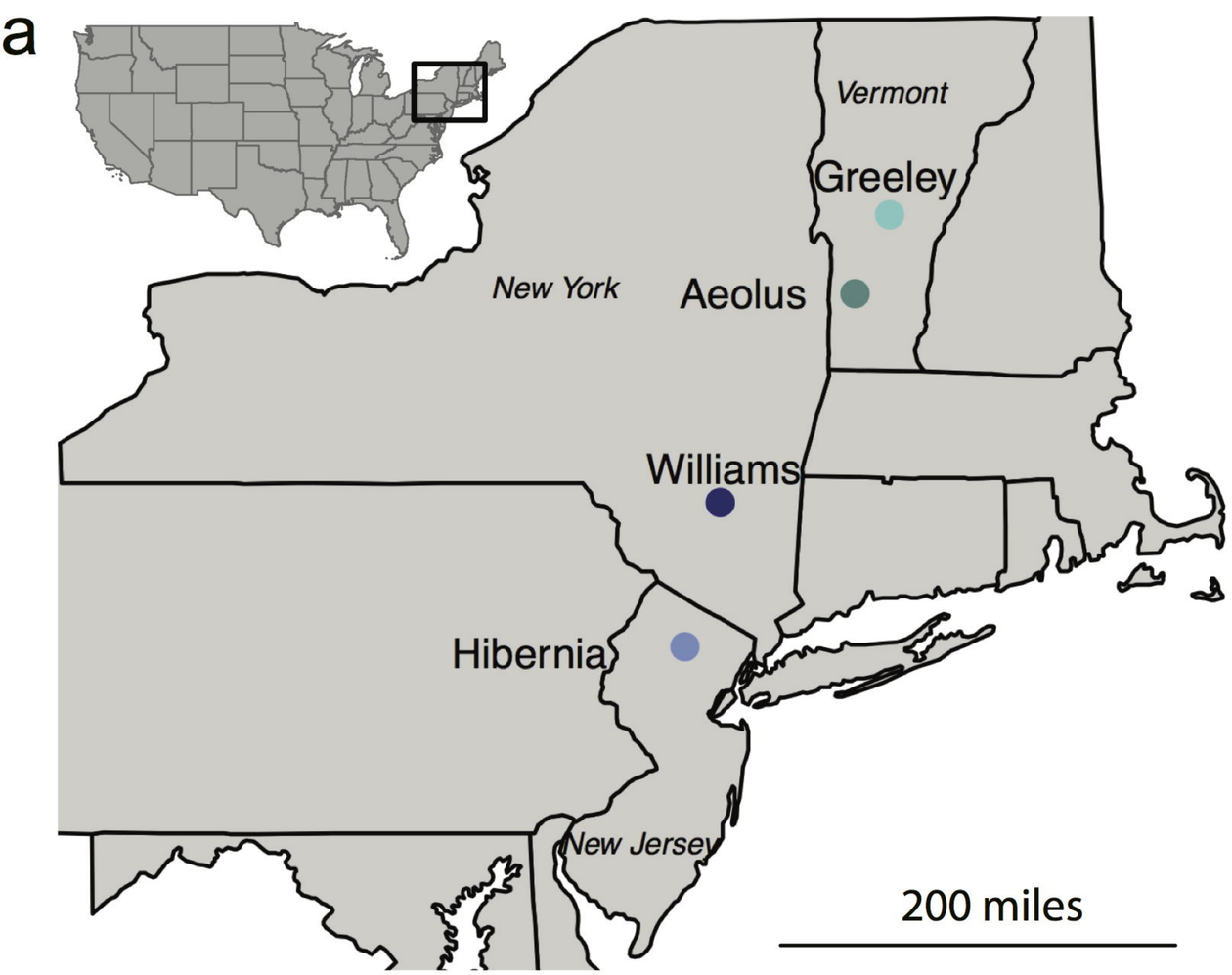
a
Vermont
Greeley
New York
Aeolus
Williams
Hibernia
New Jersey
200 miles

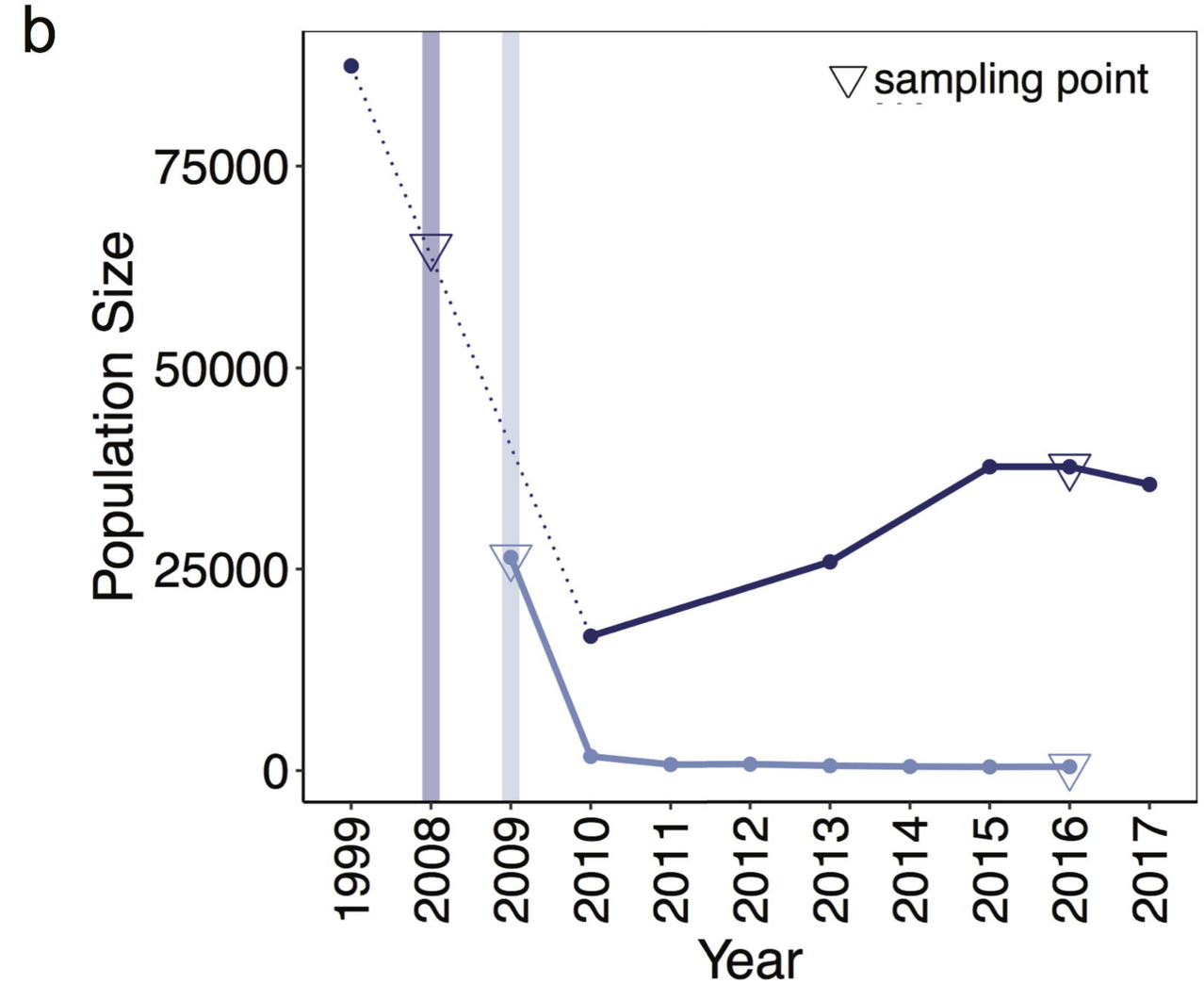
b
sampling point
Population Size
75000
50000
25000
0
1999
2008
2009
2010
2011
2012
2013
2014
2015
2016
2017
Year

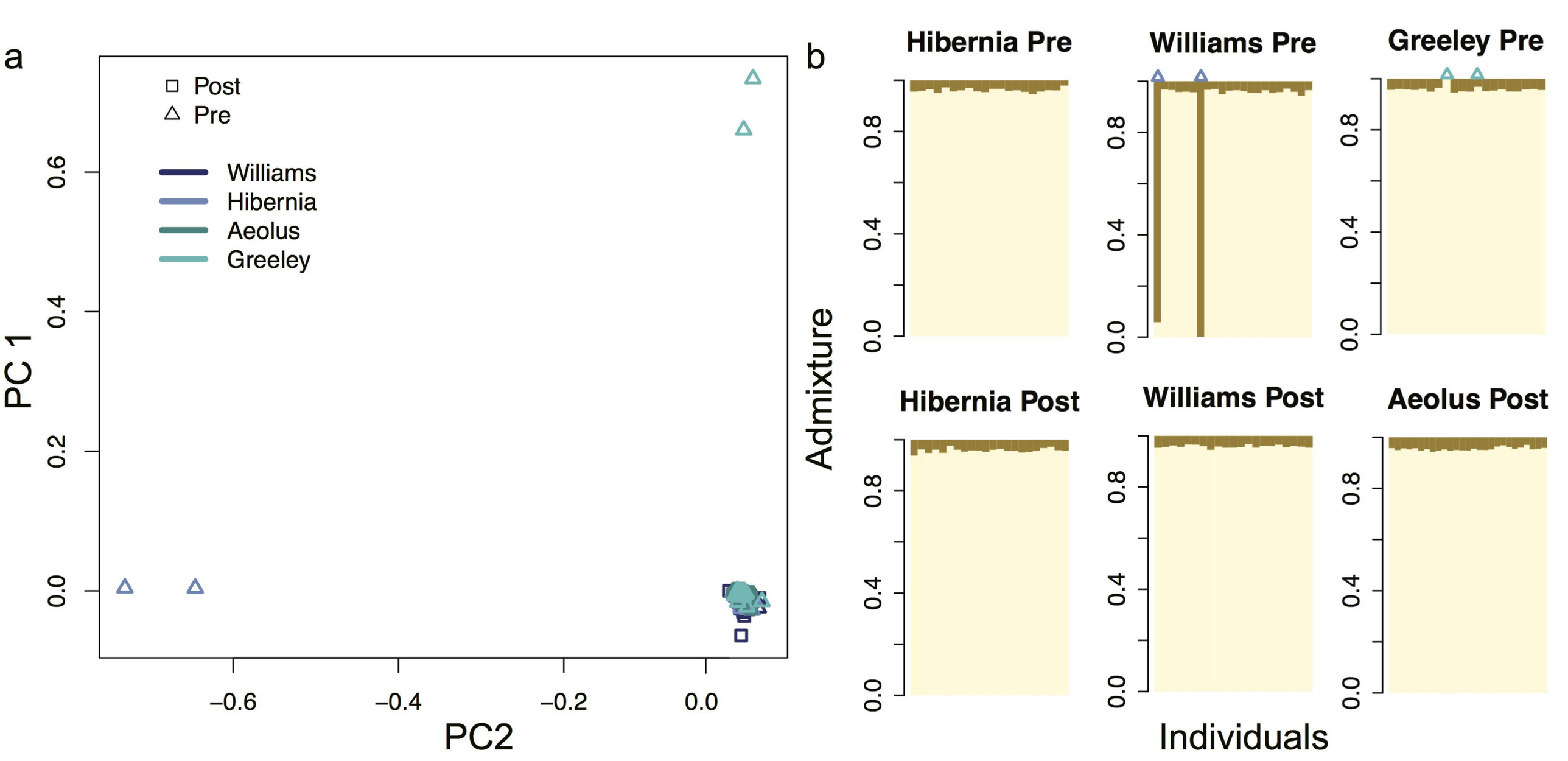
a
Post
Pre
Williams
Hibernia
Aeolus
Greeley
PC 1
PC2
0.0
0.2
0.4
0.6
−0.6
−0.4
−0.2
0.0
b
Hibernia Pre
Williams Pre
Greeley Pre
Hibernia Post
Williams Post
Aeolus Post
Admixture
Individuals
0.0
0.4
0.8

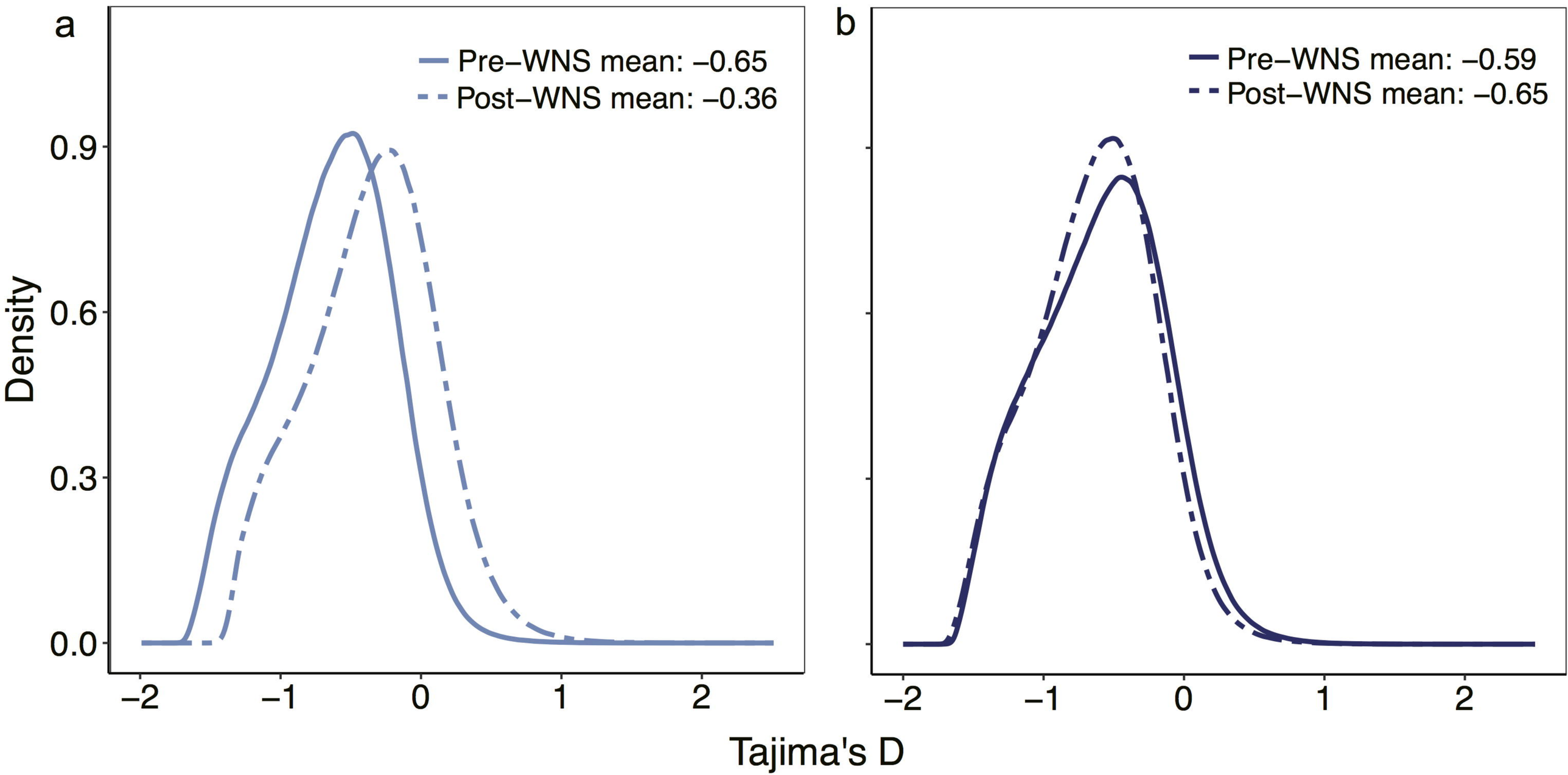
a
Pre–WNS mean: –0.65
Post–WNS mean: –0.36
b
Pre–WNS mean: –0.59
Post–WNS mean: –0.65
Density
0.0
0.3
0.6
0.9
–2
–1
0
1
2
Tajima's D

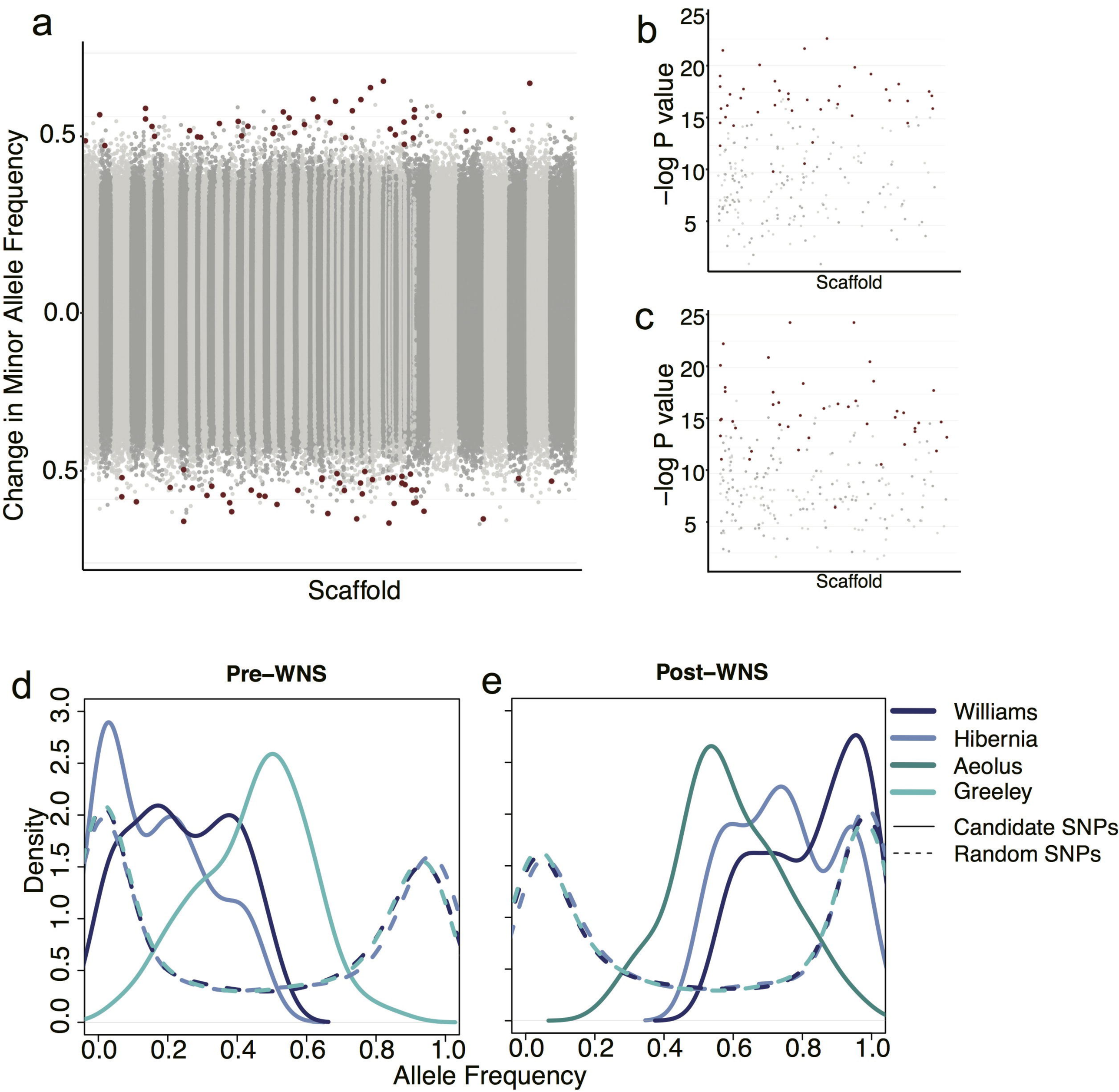
a
Change in Minor Allele Frequency
0.5
0.0
0.5
Scaffold
b
−log P value
25
20
15
10
5
Scaffold
c
−log P value
25
20
15
10
5
Scaffold
d
Pre−WNS
Density
3.0
2.5
2.0
1.5
1.0
0.5
0.0
0.0
0.2
0.4
0.6
0.8
1.0
e
Post−WNS
Williams
Hibernia
Aeolus
Greeley
Candidate SNPs
Random SNPs
Allele Frequency